

1 **Evaluating Streamflow Forecasts in Hydro-Dominated**
2 **Power Systems—When and Why They Matter**

3 **Rachel Koh¹, Stefano Galelli^{1,2}**

4 ¹Pillar of Engineering Systems and Design, Singapore University of Technology and Design, Singapore

5 ²School of Civil and Environmental Engineering, Cornell University, Ithaca, NY

6 **Key Points:**

- 7 • The benefits of streamflow forecasts trickle down from the water to the power system
8 • Forecasts are particularly useful during the transition from wet to dry seasons
9 • The relationship between forecast skill-value is controlled by the level of operational
10 integration between the two systems

Corresponding author: Rachel Koh, kohzq.rachel@gmail.com

Abstract

The value of seasonal streamflow forecasts for the hydropower industry has long been assessed by considering metrics related to hydropower availability. However, this approach overlooks the role played by hydropower dams within the power grid, therefore providing a myopic view of how forecasts could improve the operations of large-scale power systems. With the aim of understanding how the value of streamflow forecasts penetrates through the power grid, we developed a coupled-water energy model that is subject to reservoir inflow forecasts with different levels of accuracy. We implement the modelling framework on a real-world case study based on the Cambodian grid, which relies on hydropower, coal, oil, and imports from neighboring countries. In particular, we evaluate the performance in terms of metrics selected from both the reservoir and power systems, including available and dispatched hydropower, power production costs, CO₂ emissions, and transmission line congestion. Through this framework, we demonstrate that streamflow forecasts can positively impact the operations of hydro-dominated power systems, especially during the transition from wet to dry seasons. Moreover, we show that the value largely varies with the specific metric of performance at hand as well as the level of operational integration between water and power systems.

Plain Language Summary

Forecasts of river streamflow are regularly used by water system operators to plan the operations of large-scale infrastructures, such as hydropower dams. To date, research has focussed primarily on how the accuracy, or skill, of forecasts translates into added performance of reservoir systems, thereby overlooking the potential benefits for other interconnected infrastructures that depend on water availability. Here, we focus on the case on national power grids, whose performance is partially controlled by hydropower production. We show that the use of streamflow forecasts could bring benefits that ‘trickle down’ to power system operations, reducing, for instance, power production costs and CO₂ emissions during specific periods.

1 Introduction

Water managers often rely on streamflow forecasts to inform reservoir release decisions (Turner et al., 2020). As opposed to operating reservoir networks with static rule curves, streamflow forecasts offer operators the ability to dynamically adapt to anticipated inflow conditions (Troin et al., 2021). Accurate streamflow forecasts have been found to benefit multiple aspects of water management, such as flood control, water supply reliability, or hydropower production (Nayak et al., 2018; Delaney et al., 2020). The metrics used to assess the benefits, or value, of streamflow forecasts can be broadly classified under two categories. Under the first category, benefits are defined in terms of deviations from a pre-defined target, usually the target storage or release (Li et al., 2014; Turner et al., 2017). Under the second category, benefits are defined through metrics measuring the improvement in performance with respect to one or multiple objectives. Examples include reduction in water shortage (Nayak et al., 2018) or spilled water volume (Anghileri et al., 2016), better flood control (Wang et al., 2012; Galelli, Goedbloed, et al., 2014), and hydropower generation or revenue (Anghileri et al., 2019; Ahmad & Hossain, 2020; Doering et al., 2021; Guo et al., 2021; Lee et al., 2022). The common denominator among these metrics is that they are based on the output produced by a reservoir system model.

In hydro-dominated power systems, reservoir operations can have profound effects on power system operations (Voisin et al., 2020; Chowdhury et al., 2021; Chowdhury, Dang, et al., 2020). During dry conditions, for instance, a decrease in hydropower production may force power grid operators to raise production from thermolectric plants, leading to higher operating costs and CO₂ emissions (Kern et al., 2020; Chowdhury et al., 2021). Defining streamflow forecast value solely in terms of water-related metrics thus overlooks the role

61 played by hydropower reservoirs in the power grid. In this regard, it is worth stressing that
 62 there are only a handful of studies that evaluated whether the use of streamflow forecasts
 63 brings value to power grid operations (Ding et al., 2021; Gong et al., 2021). Both studies
 64 were conducted at the scale of a river basin—rather than on a spatial domain encompassing
 65 a national or regional grid—and adopted performance metrics defined in terms of power
 66 production only (i.e., supply from hydropower, wind, and solar photovoltaic). Hence, an in-
 67 depth understanding of how power system operations could benefit of streamflow forecasts
 68 is missing. In particular, it is important to understand which performance metrics are
 69 improved by the use of streamflow forecasts, when forecasts are most useful, and how forecast
 70 skill translates into different performance metrics. All these aspects would indeed be relevant
 71 to support the operationalization of streamflow forecasts.

72 Here, we aim to advance the current body of knowledge by studying how the value
 73 of streamflow forecasts unfolds as we move beyond a water reservoir system to include the
 74 operations of a national power grid. The questions of interest are therefore the following:
 75 How does forecast value change as we consider different performance aspects of a power
 76 grid? When is the use of forecasts more beneficial? How does forecast skill affect power
 77 system operations? Is forecast value affected by the interdependencies of the water-energy
 78 system? With the aid of a reservoir and power system model, we answer these questions
 79 by evaluating the value of streamflow forecasts for the operations of the Cambodian power
 80 system, which largely relies on the hydropower sector (Section 2 and 3). The criteria used
 81 in such evaluation are multiple metrics taken from both the reservoir and power systems,
 82 including available hydropower, dispatched hydropower (i.e., hydropower used within the
 83 grid), power production costs, CO₂ emission, and transmission line stress (Section 4). By
 84 simulating the coupled water-energy system with and without streamflow forecasts, we show
 85 that forecasts are particularly useful during the transition from the summer monsoon to the
 86 dry season. We also quantify the relationship between forecast skill and value, and show
 87 that forecast error is less important for production costs and CO₂ emissions, which are also
 88 impacted by electricity demand. We finally study how different levels of integration between
 89 water and power systems reshapes the skill-value relationship (Section 5).

90 **2 Case study and Data**

91 **2.1 Case study**

92 We carried out our analysis on the Cambodian water-energy system, illustrated in Fig-
 93 ure 1. The representation of the system is based on the infrastructure built and operated
 94 in 2016, for which detailed data are available (Chowdhury, Kern, et al., 2020). Power sup-
 95 ply is largely controlled by a network of six hydropower dams, which have a total installed
 96 capacity of 1,048 MW (see Table 1). In this reservoir network, there are two embankment
 97 dams (Kirirom I and Kirirom III), two dams operated in cascade (Atay and LR Chrum),
 98 and two headwater dams (Kamchay and Tatay). As we shall see, their production shows
 99 a pronounced inter-annual pattern; production increases during the summer monsoon (typ-
 100 ically between May and October) and decreases during the dry season. The hydropower
 101 production is complemented by a few additional resources, namely thermoelectric plants
 102 (three coal-fired units totaling 400 MW of installed capacity and 15 oil-fired units totaling
 103 282 MW), and import from neighboring countries (Thailand, Laos, and Cambodia). Taken
 104 together, all these resources are designed to meet the peak demand of 1,068 MW (EDC,
 105 2016).

106 **2.2 Data**

107 Different datasets were obtained as inputs to the reservoir and power system models.
 108 Inputs to reservoir system model include reservoir specifications (Table 1) and time series
 109 of observed inflow and inflow forecasts. Since long and reliable time series of observed
 110 river discharge are not available, we retrieved inflow data for the six reservoirs from the

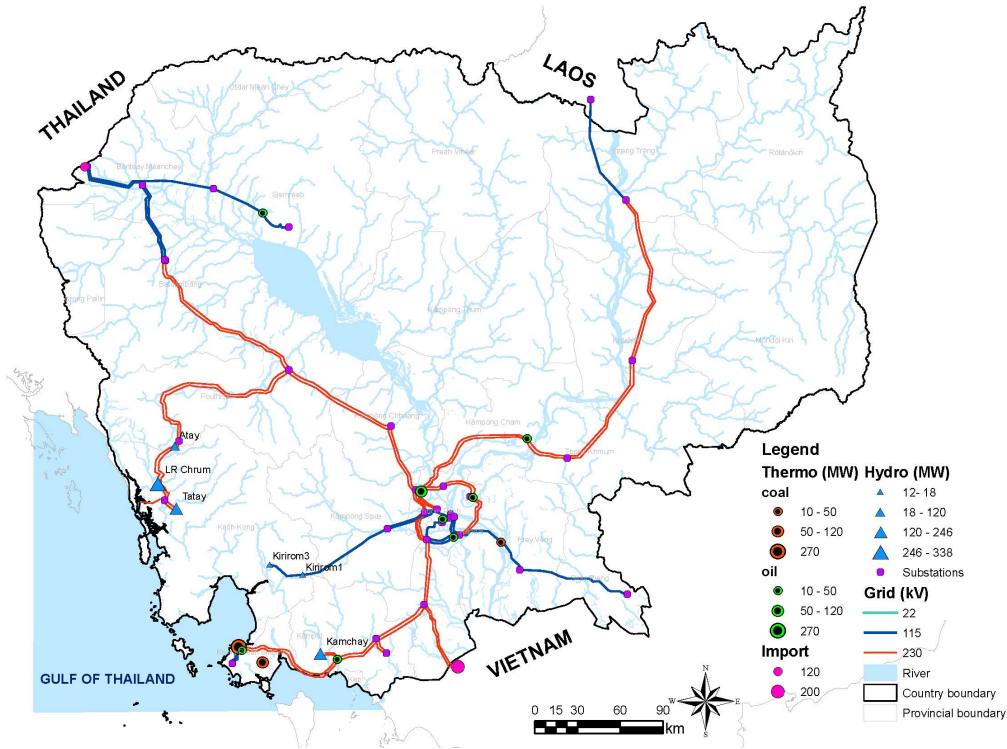


Figure 1. Main components of the Cambodian water-energy system, as of 2016. The circles represent the thermoelectric plants (coal and oil) and imports from neighbouring countries, while the triangles represent the hydropower plants. The purple squares and segments denote the substations and transmission lines, respectively. The river network is shown in light blue. Further details are provided in Section 2.1

Table 1. Design specifications of the Cambodian hydropower dams (EDC, 2016).

Name	Installed capacity (MW)	Dam height (m)	Storage (Mm ³)	Design discharge (m ³ /s)	Hydraulic head (m)	Basin area (km ²)
Kamchay	194.1	110	680	163.5	122	710
Kirirom I	12	34	30	20	373.5	99
Kirirom III	18	40	30	40	271	105
Atay	240	45	443.8	125	216	1,157
LR Chrum	338	68	62	300	132	1,550
Tatay	246	77	322	150	188	1,073

111 Global Flood Awareness System (GloFAS) (Harrigan et al., 2021), a data source that (i) is
 112 commonly used in developing Asian countries (MacLeod et al., 2021) and (ii) allows us to
 113 model the water-energy system with a reasonable degree of accuracy (Koh et al., 2022). For
 114 consistency, we adopted the streamflow forecasts issued by GloFAS, which consists of an
 115 11-member ensemble (Zsoter et al., 2020). The inflow data are available from 1979 to near
 116 real-time with daily resolution. Inflow forecasts are available for two days weekly (every
 117 Monday and Thursday) with a 24-hour time step and up to 46-day lead time. Forecasts

118 are available from January 1999 to December 2018. The common period (2000-2018) was
119 selected for all experiments.

120 For the power system model, required data include the specifications of the trans-
121 mission lines and generators, as well as hourly time series of electricity demand at each
122 substation. The line and generator details were extracted from technical reports (EDC,
123 2016; JICA, 2014), while the monthly peak demand was retrieved from the same reports.
124 Based on the available monthly peak demand and hourly demand profiles for weekdays and
125 weekends, we distribute the national demand to each substation on the basis of its voltage
126 level. The detailed methodology for deriving the electricity demand time series is reported
127 in Koh et al. (2022).

128 **3 Modelling framework**

129 **3.1 Overview**

130 As illustrated in Figure 2, the components of our computational framework are (1) a
131 reservoir system model, (2) a power system model, and (3) a reservoir re-operation model.
132 Note that the ‘typical’ representations of water-energy models include only the first two
133 components: the reservoir model releases water according to its operating rules, and the
134 amount of available hydropower is communicated to the power system model, which then
135 dispatches (part of) the available hydropower depending on the specific dynamics of the
136 power grid. This approach of separately modelling the water and power systems with a
137 one-way information flow is known as ‘soft-coupling’ (Voisin et al., 2006; Chowdhury, Kern,
138 et al., 2020; Kern et al., 2020). In our framework, we also use a reservoir re-operation model
139 that explicitly accounts for the feedback from the power to the water system. In particular,
140 the re-operation model gathers information on the amount of hydropower dispatched into the
141 grid and calculates the corresponding amount of water that should be released from the dams
142 (more details in Section 3.4). By engaging this component, the reservoir and power system
143 models are ‘hard-coupled’, thus representing a situation in which the reservoir operations
144 are contingent upon the state of the power system (Ibanez et al., 2014; Gebretsadik et al.,
145 2016; Koh et al., 2022).

146 In our study, we evaluate the value of streamflow forecasts in the Cambodian grid by
147 first operating the system with the soft-coupling approach. Doing so has two advantages.
148 First, the unidirectional information flow provides insights into how the value of streamflow
149 forecasts changes as we move from performance metrics focussing on the reservoir system to
150 metrics focussing on the power system. Second, the lack of a tight operational integration
151 between the two systems yields a larger operating space, allowing us to identify stressors
152 (e.g., forecast skill) that control system performance—and that could be ‘masked’ by the
153 presence of the feedback between the energy and water system. In the second part of our
154 experiments, we incorporate the feedback mechanism between the systems by introducing
155 the reservoir re-operation model. This adds one more stage to the modelling process, where
156 the amount of hydropower dispatched by the power system is communicated back to the
157 reservoir system model. Doing so provides insights into how the role played by streamflow
158 forecasts within the power grid changes when the operating space is reduced.

159 **3.2 Reservoir system model**

160 The daily amount of hydropower available at each reservoir is determined by the reser-
161 voir system model through its release decisions, which can be determined by two alternative
162 schemes: (i) a benchmark one based on static rule curves, and (ii) a more complex scheme
163 that dynamically integrates the streamflow forecasts.

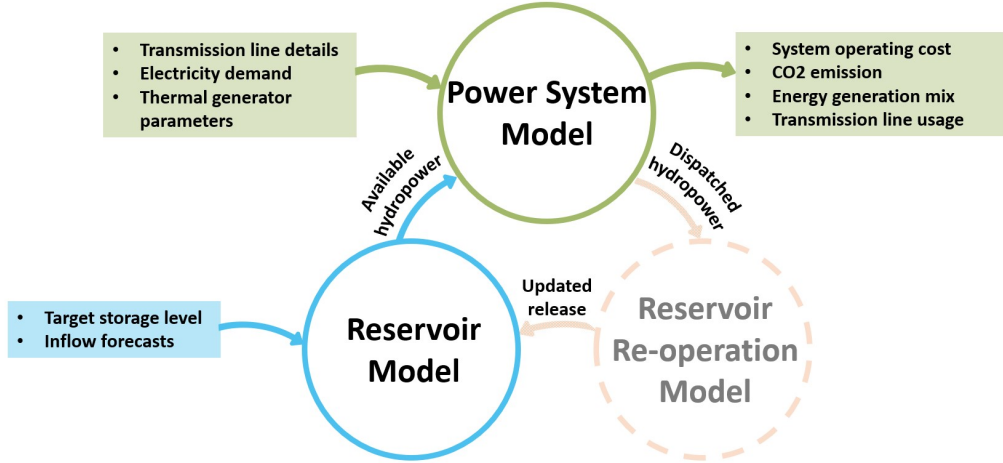


Figure 2. Schematic of the computational framework, comprising a reservoir system model, a power system model, and a reservoir re-operation model. The arrows represent the information flow between modelling components. The circles for the reservoir and power system models are in solid lines to represent the fact that these components are ‘typically’ considered in water-energy studies, where a water model provides the boundary conditions for a power system model. The dashed circle around the re-operation model indicates that this is an optional model that can be engaged when needed.

164 **3.2.1 Benchmark scheme: rule curves**

165 The storage dynamics of the i -th reservoir are described by the following mass balance,
 166 solved with a daily time step:

$$\begin{aligned}
 S_d^i &= S_{d-1}^i + Q_d^i - R_d^i - spill_d^i - E_d^i, \\
 0 &\leq S_d^i \leq S_{cap}^i, \\
 Q_{MEF,d}^i &\leq R_d^i \leq R_{max}^i,
 \end{aligned}
 \tag{1}$$

167 where S_d^i is the reservoir storage on day d , Q_d^i the reservoir inflow (between day $d - 1$ and
 168 d), R_d^i the volume of water released through the turbines, $spill_d^i$ the volume of water spilled
 169 from the reservoir, E_d^i the evaporation losses from the dam, and S_{cap}^i the capacity of the
 170 dam.

171 An example of the rule curves we adopted is illustrated in Figure S1 (in the SI). Each
 172 rule curve is composed of a piecewise linear function based on the maximum and minimum
 173 water levels that the reservoir should reach within a calendar year (H_1^i and H_2^i) and the
 174 time of year in which these values should be reached (T_1^i and T_2^i). The concept of defining
 175 reservoir operating rule curves in this manner was proposed by Oliveira and Loucks (1997)
 176 and subsequently adapted in several other studies (e.g., Liu et al. (2011); Yassin et al.
 177 (2019)). Its use in representing actual system operations in Southeast Asia has also been
 178 validated (Chowdhury, Kern, et al., 2020; Dang et al., 2020). As an offline operating policy,
 179 the daily release decision R_d^i is made to bring the actual storage as close to the target storage
 180 as possible, while being subjected to an upper bound (R_{max}^i) and lower bound ($Q_{MEF,d}^i$).
 181 R_{max}^i is the maximum volume of water that can be turbined (representing the designed
 182 discharge capacity of the dam), while $Q_{MEF,d}^i$ represents the downstream environmental
 183 flow requirement, calculated according to the method used in Pastor et al. (2014).

184 Finally, the daily available hydropower for the i -th reservoir is calculated as follows:

$$HP_d^i = \eta \times \rho \times g \times R_d^i \times (H_{d-1}^i + H_d^i)/2, \quad (2)$$

185 where HP_d^i is the available hydropower (MW) on day d , η the turbine efficiency, ρ the water
 186 density (1000 kg/m³), g the gravitational acceleration (9.81 m/s²), and H_d^i the hydraulic
 187 head, taken as the average between days $d - 1$ and d . For dams operated in cascade, Eq.
 188 (1) is updated to account for the natural inflow as well as the turbined and spilled water
 189 from the upper reservoir(s).

190 3.2.2 Forecast-informed scheme

191 In contrast to the benchmark scheme—where the reservoir release is only contingent
 192 upon the target water level—operating with streamflow forecasts allows the operators to
 193 make release decisions based on the knowledge available for the future inflows. In turn, this
 194 allows the system to prepare for impending wet or dry events. To integrate this information,
 195 the reservoir operation scheme employs a deterministic Model Predictive Control (MPC)
 196 approach (Galelli, Goedbloed, et al., 2014; Turner et al., 2017; Lee et al., 2022). According
 197 to this scheme, at the beginning of day d , the model receives a deterministic streamflow
 198 forecast for the next H days for each reservoir i ($Q_d^{f,i}, \dots, Q_{d+H-1}^{f,i}$), and optimizes the
 199 release over that finite horizon (i.e., days $[d, d + H - 1]$) according to a pre-defined objective
 200 function. In our work, consistent with the operating rules, we seek to explicitly maximize
 201 the hydropower generated by each dam. To prevent an over-aggressive release profile, we
 202 impose a penalty on the final state of the reservoir storage at the end of the forecast horizon
 203 (Soncini-Sessa et al., 2007), ensuring that it does not deviate too much from the target
 204 water levels (Figure S1). This yields the following optimization problem for each reservoir
 205 i :

$$\max_{R_d^i, R_{d+1}^i, \dots, R_{d+H-1}^i} \sum_{t=d}^{d+H-1} HP_t^i - X(s_{t=d+H-1}^i), \quad (3)$$

206 where HP_t^i is the amount of hydropower produced by the i -th reservoir in one day and
 207 $X(\cdot)$ is the penalty associated to the storage on day $(d + H - 1)$. HP_t^i is derived from
 208 Eq. (2) as a result of iteratively solving, over H days, Eq. (1) with Q_d^i replaced by the
 209 streamflow forecast $Q_d^{f,i}$. The release decisions are thus bounded by $Q_{MEF,d}^i$ and R_{max}^i . The
 210 output of the optimization problem (block of H days) is a time series of release decisions
 211 $R_d^i, R_{d+1}^i, \dots, R_{d+H-1}^i$. Contingent upon the actual inflow (Q_d^i), we implement the release
 212 for the first day (R_d^i), and calculate the mass balance for each reservoir according to Eq. (1).
 213 The actual hydropower produced (HP_d^i) derived through Eq. (2) is then communicated
 214 to the power system model for dispatch. In sum, prior to each day d , we solve multiple MPC
 215 problems (one for each hydropower reservoir) with the aim of maximizing the hydropower
 216 generation for each reservoir over the next H days, yielding a sequence of reservoir releases
 217 as decision variables ($R_d^i, R_{d+1}^i, \dots, R_{d+H-1}^i$).

218 3.3 Power system model

219 The power system model is PowNet, a production cost model that solves a mixed
 220 integer linear program with the objective of fulfilling the hourly electricity demand at min-
 221 imum cost (Chowdhury, Kern, et al., 2020). The decisions made by PowNet include, for
 222 the next 24 hours, (i) which generating units to start-up and shut down (unit commitment)
 223 and (ii) the amount of power supplied by each unit (economic dispatch). Key inputs to
 224 PowNet include transmission line parameters, hourly time series of electricity demand at
 225 each sub-station, techno-economic parameters of thermoelectric generators (e.g., capacity,
 226 operations and maintenance costs), and the hydropower available at each dam calculated by
 227 the reservoir system model (Section 3.2). In scheduling the hourly production, the model
 228 is subject to multiple constraints, including ramping limits, generation limits, minimum up
 229 and down-time of each generator, and transmission capacity constraints. The decision vari-
 230 ables at each hour thus include binary variables (e.g., generating unit to use and whether

to switch it on or off) and continuous ones (e.g., electricity generated by each unit, voltage angle at each node, spinning and non-spinning reserves, amount of renewables and imports dispatched). For each simulated day, PowNet outputs include hourly time series of operating costs, CO₂ emissions, generation mix, and transmission line usage. PowNet has been applied to multiple national grids, such as the ones of Cambodia (Chowdhury, Kern, et al., 2020), Laos (Chowdhury, Dang, et al., 2020), and Thailand (Chowdhury et al., 2021; Galelli et al., 2022).

3.4 Reservoir re-operation model

The reservoir re-operation model is introduced as a means to capture the feedback between interdependent water-energy systems. Serving as a bridge between the reservoir and power system, this model compares the amount of available hydropower produced by the i -th reservoir (HP_d^i) with the amount dispatched by the power system (HP_d^{i*}). With the goal of reducing the mismatch between these two values, the re-operation is triggered when there is an over-production of hydropower (i.e., $HP_d^{i*} < HP_d^i$). The re-operation algorithm (refer to Koh et al. (2022) for details) then re-calculates the reservoir release such that the i -th reservoir releases only the amount R_d^{i*} ($< R_d^i$) needed to produce HP_d^{i*} . In this study, all reservoirs are re-operated in the scenario where the feedback between the systems is considered. Operating in this manner offers flexibility whereby the release decisions made by the hydropower reservoir can be updated based on real-time information regarding the power system. In other words, this allows each reservoir to be used as a ‘battery’, so water can be stored for future use. Doing so may alter the value of forecasts, as the operations of the reservoirs would then depend on the state of the power system as well.

4 Experimental setup

The goal of our study is to quantify the value of streamflow forecasts for power system operations, understand how the value changes with skill, and determine when the value matters the most. We use multiple benchmarks to characterize system operations under different conditions and thus meet our goals. First, we use the benchmark scheme (Section 3.2.1), i.e., static rule curves, to characterize reservoir operations. Subsequently, we compare the results to the forecast-informed scheme. Here, we introduce two benchmarks, perfect forecasts and climatology, both commonly used to assess the value of streamflow forecasts (Grantz et al., 2005; Zhao et al., 2012; Yossef et al., 2013; Zimmerman et al., 2016; Nayak et al., 2018; Anghileri et al., 2019; McNerney et al., 2020; Quedi & Fan, 2020). To characterize the skill-value relationships, we have at our disposal multiple forecasts within the ensemble, so one could perform weighted aggregation on the members or consider each member as a separate deterministic forecast (Slater et al., 2016; Delaney et al., 2020). We consider both, that is, (i) we take the ensemble mean across the 11 members (more details in Section 2.2), and (ii) we use the individual members as independent inputs. In sum, we run our simulations under 14 different forecast scenarios—i.e., perfect forecasts, climatology (taken as a 365-calendar day average from the inflow data), ensemble mean, and each of the 11 members. Taking into account how system operations may depend on the state of the power system as well, we repeat the experiments with the feedback from the power system back to the reservoir model. This means that our experiments are conducted (i) with 14 different deterministic forecast scenarios, and (ii) without and with feedback.

The forecast horizon selected in our study is 30 days based on the power generation mix obtained by preliminarily testing the system operations with different forecast horizons (see Table S1 in the SI for additional details). Since the reservoirs in our model are operated at the daily time step while the forecasts are only available on every Monday and Thursday of each week (Zsoter et al., 2020), we fill the gaps (Tuesday-Wednesday, Friday-Sunday) by extracting a 30-day window from the 46-day availability, and shifting the forecast one-day ahead, until the next set of forecasts is available. For example, the forecast for a given

Monday would be from day 1 to day 30 (out of the available 46 days), and the forecast for Tuesday would be from day 2 to 31 for the same set of 46 days. This is repeated for Wednesday; on Thursday, a new set of forecast is available again. Based on simulations ran on an Intel(R) Core (TM) i7-8700 CPU 3.2 GHz with 8 GB RAM running Windows 10, the runtime is approximately 20 hours for each simulation. The total runtime for 14 scenarios is thus approximately 280 hours. The experiments including the feedback from the power to the water system are more computationally demanding, taking about 40 hours each to complete.

Moving to the specific metrics that can be used to quantify forecast skill for deterministic forecasts, it is worth stressing that the options are many (Huang & Zhao, 2022). In this study, we considered the use of the Nash-Sutcliffe efficiency (NSE) (Nash & Sutcliffe, 1970), Pearson correlation coefficient (Lima & Lall, 2010; Li et al., 2014) and Symmetric Mean Absolute Percentage Error (SMAPE) (Ogliari et al., 2021). Since the forecast skill is calculated for each reservoir within the system, a spatial aggregation is necessary to represent the overall skill for the entire study area and contrast it against performance metrics defining forecast value (e.g., CO₂ emissions). The primary criterion for the chosen metric is that it has to be bounded to prevent skewed values upon aggregation, thus eliminating NSE $(-\infty, 1]$ as a candidate. As for the Pearson correlation coefficient, there is a possibility of positive and negative values cancelling each other out during the aggregation process, thus misleading both the strength and direction of the relationship between the actual and forecast time series. SMAPE is an accuracy metric that measures the difference between the actual and forecast data between 0 and 1, and is a metric that fulfills both requirements for our study. All candidate metrics are illustrated in Figure S2; across the reservoirs, forecast errors tend to be larger during the pre-monsoon (Feb-Apr). The skill then progressively increases until the end of the year. To derive the overall skill of a forecast member across space, we perform a weighted average of the errors with respect to the hydropower plant capacities following Eq. (4):

$$SMAPE_d = \sum_{i=1}^N (w_i * SMAPE_{i,d}), \quad (4)$$

where $SMAPE_d$ is the aggregated forecast error on day d , w_i is the weight of the i -th reservoir, taken as the hydropower capacity divided by the total capacity of the N reservoirs, and $SMAPE_{i,d}$ is the forecast error for the i -th reservoir on day d .

As for the forecast value, we consider six metrics: the available, dispatched, and unused hydropower, system operating costs, CO₂ emissions, and the number of N-1 violations—i.e., instances in which any of the high-voltage lines reaches 75% of its capacity—an indicator of grid stress. Here, note that the available hydropower is an output of the reservoir system model (derived through Eq. (2)), a commonly-used metric to assess forecast value in previous studies (Lee et al., 2022; Anghileri et al., 2019). The other metrics are produced by the power system model, and are thus chosen to represent multiple performance aspects of the grid. First, the hydropower metrics provide insights into how forecast value is transferred from the water system to the power system. Next, the system operating costs and CO₂ emissions provide insights into how system operations are impacted by different levels of forecast accuracy. Last, the N-1 violations indicate how stressed the transmission lines are. This is important, since (i) grid stress is considered one of the triggers for blackouts (Veloza & Santamaria, 2016), and (ii) can serve as an indicator of system performance (e.g., when line capacity limits the penetration of renewables in the grid (Chowdhury, Dang, et al., 2020)). In assessing the skill-value relationship, we note that there are other input variables (from both the reservoir and power system) that may influence the overall system performance. As such, besides forecast skill, the actual inflow (Q) and the electricity demand are also considered as system stressors.

5 Results

In this section, we first evaluate the benefits that lie in adopting streamflow forecasts when operating hydro-dominated power systems (Section 5.1). This is done by comparing results obtained from simulating the reservoir and power systems under different benchmark operating schemes. Then, we investigate how the value of forecasts changes with skill (Section 5.2). Here, we investigate the skill-value relationship under both standard operations (i.e., without feedback; Section 5.2.1) and operations with feedback between the power and water systems (Section 5.2.2). Such comparison illustrates how the value changes as we capture the interdependencies between water and power systems.

5.1 Value of streamflow forecasts

5.1.1 Comparison across multiple performance metrics

To determine the value of streamflow forecasts in power system operations, we aggregate the five key performance metrics across both space and time (since the reservoir model is run with a daily time-step and the power system model with an hourly time-step). The metrics include system-wide available and dispatched hydropower, system operating costs, CO₂ emissions, and number of N-1 violations (Figure 3). For comparison, we include the results for operations guided by rule curves and three different forecast-informed schemes, namely perfect forecasts, climatology, and the ensemble mean. At the monthly timescale, a strong seasonal pattern can be observed across all metrics. Despite the similar pattern exhibited by the different operating schemes, it is clear that the use of streamflow forecasts affects the operations of both reservoir and power system.

5.1.1.1 Available hydropower. Temporally, the system behavior can be classified into three periods, namely pre-monsoon (Feb-Apr), summer monsoon (May-Oct), and post-monsoon (Nov-Jan). The value of streamflow forecasts largely varies across these periods. We first focus on the amount of available hydropower, a direct product of the reservoir system model (boxplot in the top panel of Figure 3). Across all scenarios, the hydropower availability increases from the pre-monsoon to peak at the end of the monsoon, before decreasing again. This follows the seasonal pattern of the summer monsoon, a key feature of Southeast Asian climates (Chowdhury et al., 2021). Operating the reservoirs using rule curves results in larger hydropower availability than the schemes with forecasts during the pre-monsoon and monsoon period (see the corresponding mean and standard deviation in Table 2). During the monsoon, operating the dams without streamflow forecasts generates an average of at least 40 GWh more hydropower each month than the other schemes. This result is attributed to the nature of the decisions made with rule curves: without forecast, the release decisions of each reservoir are made with respect to the target storage only. As such, the reservoirs tend to release water whenever they receive large inflow volumes, resulting in large hydropower availability. Consequently, after the monsoon, the reduced inflow also causes the reservoirs to make smaller releases. The hydropower availability thus drops significantly (by 40–60% from November to December), averaging at least 60 GWh/month less than the forecast-informed schemes. In other words, this sharp decline is due to the myopic nature of the rule curves. In contrast, operating with forecasts allows the reservoirs to maintain a larger hydropower production after the monsoon. Looking at the specific forecast-informed schemes, we observe that operating with perfect foresight produces the best results throughout all seasons—a result that is consistent with past studies (Anghileri et al., 2019; Ahmad & Hossain, 2020; Doering et al., 2021; Guo et al., 2021; Lee et al., 2022).

5.1.1.2 Power-related metrics. The circles in the top panel of Figure 3 represent the hydropower dispatched within the grid. The first point to make is that not all available hydropower is dispatched by the grid. The mismatch between available and dispatched hydropower is accentuated during the monsoon season, when the amount of dispatched hy-

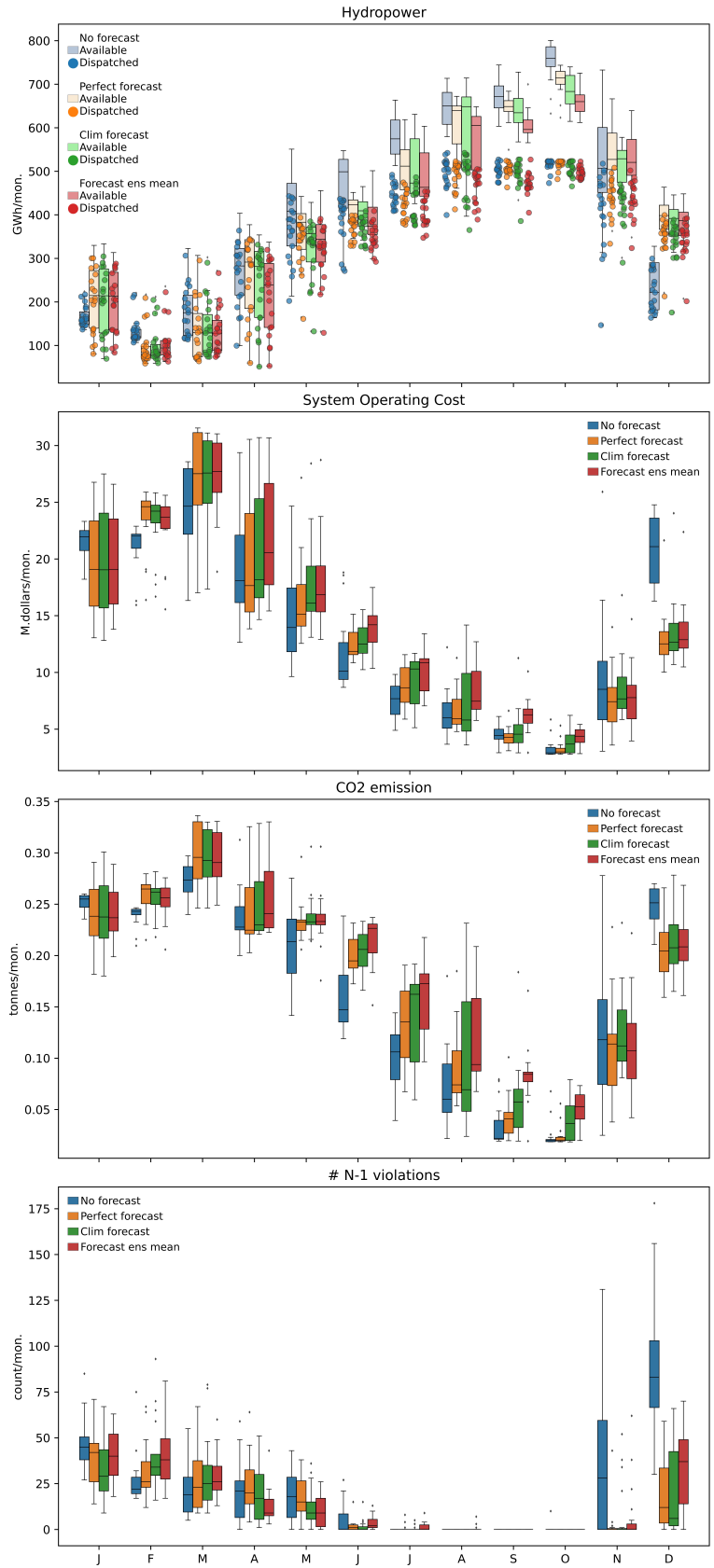


Figure 3. Monthly variability in system performance under different forecast-informed schemes. The four panels illustrate the range of variability in hydropower (available and dispatched), system operating costs, CO₂ emissions, and frequency of N-1 violations, respectively. All variables are spatially aggregated across the entire power system. Within each panel, the results from three forecast-informed schemes (perfect forecasts, climatology, and ensemble mean) are compared to the benchmark (no forecasts). Experiments are conducted without feedback between the reservoir and power systems.

Table 2. Variability in mean and standard deviation of the performance metrics illustrated in Figure 3 across different operating schemes (no forecasts, perfect forecasts, climatology and ensemble mean) and periods (pre-monsoon, monsoon and post-monsoon).

Performance metric	Scenario	Pre-monsoon	monsoon	Post-monsoon
Available hydropower (GWh/mon.)	No forecasts	195.16± 83.11	584.51±137.29	302.19±173.18
	Perfect forecasts	164.98±101.99	539.87±136.00	377.93±151.97
	Climatology	159.95± 91.11	527.80±142.82	360.75±142.47
	Ensemble mean	151.60± 78.62	506.85±132.20	366.82±146.94
Dispatched hydropower (GWh/mon.)	No forecasts	191.04± 76.31	451.26±71.55	267.27±120.78
	Perfect forecasts	160.62±94.75	439.50±76.23	329.83±114.60
	Climatology	157.17±86.50	431.12±82.74	319.20±111.61
	Ensemble mean	149.58±75.94	415.42±77.53	323.97±113.65
Unused hydropower (GWh/mon.)	No forecasts	4.12± 8.12	133.26± 69.40	34.92± 55.00
	Perfect forecasts	4.36± 8.57	100.37± 62.29	48.10± 40.90
	Climatology	2.78± 5.62	96.68± 62.58	41.54± 33.51
	Ensemble mean	2.02± 3.65	91.42± 56.61	42.85± 36.16
System operating cost (M.dollars/mon.)	No forecasts	21.58± 4.13	8.02± 4.70	17.28± 6.65
	Perfect forecasts	23.47± 5.21	8.67± 4.99	13.34± 5.91
	Climatology	23.68± 4.81	9.17± 5.39	13.99± 5.79
	Ensemble mean	24.16± 4.42	10.11± 5.12	13.70± 5.87
CO ₂ emission (tonnes/mon.)	No forecasts	0.25± 0.02	0.10± 0.07	0.21± 0.07
	Perfect forecasts	0.27± 0.04	0.12± 0.08	0.18± 0.07
	Climatology	0.27± 0.03	0.13± 0.08	0.19± 0.06
	Ensemble mean	0.27± 0.03	0.14± 0.07	0.19± 0.07
# N-1 violations (hours/mon.)	No forecasts	22.96± 15.00	3.98± 9.32	59.16± 40.45
	Perfect forecasts	27.70± 15.67	3.39± 7.78	20.07± 21.10
	Climatology	30.00± 19.83	2.42± 6.13	20.65± 21.05
	Ensemble mean	27.63± 17.32	2.76± 5.42	26.21± 22.36

379 dropower not does not increase with hydropower availability. In fact, its value stabilizes
 380 around 450 GWh/month, leading to a larger discrepancy between the two metrics. This
 381 indicates a condition of over-production, a situation in which the grid is unable to dis-
 382 patch all the available hydropower due to oversupply or limited transmission capacity. The
 383 percentage of total dispatched hydropower with respect to the total available for the four
 384 scenarios (no forecasts, perfect forecasts, climatology, and ensemble mean) over 19 years is
 385 81.7%, 84.4%, 84.9%, and 85.1%, respectively. The discrepancy peaks at the end of the
 386 monsoon season, with up to 35%, 29%, 29%, and 28% of hydropower unused in the four
 387 scenarios, respectively. This indicates that defining value in terms of different performance
 388 metrics can produce varying conclusions. The current practice of defining value in terms
 389 of available hydropower (determined by a water system model), may therefore overlook the
 390 disparity between the available and dispatched hydropower, especially during the monsoon.
 391 To achieve a comprehensive understanding of streamflow forecast values, it is therefore im-
 392 portant to evaluate the responses of multiple performance metrics spanning across water
 393 and power systems.

394 With the largest installed capacity in the grid (about 50%), hydropower fulfills more
 395 than half of the overall electricity demand in Cambodia. The amount of hydropower within
 396 the system thus plays a paramount role in determining the power system operations and the
 397 energy generation mix (refer to Figure S3 in the SI), which directly affects operating costs
 398 and CO₂ emissions. Referring to the second and third panel in Figure 3, an observation
 399 similar to the case of hydropower can be made; the benefits of operating with forecasts
 400 are accentuated during the post-monsoon season. Towards the end of the monsoon (in
 401 October), the scheme with perfect forecasts outperforms all other scenarios in terms of
 402 operating costs, and is comparable to the case without forecasts in terms of CO₂ emissions.
 403 This suggests that while the use of forecasts may not be very beneficial to the system during
 404 the pre-monsoon and the peak of the monsoon, given the right conditions, a better forecast
 405 can be advantageous from an earlier point in time to achieve lower operating costs and CO₂
 406 emissions. A larger amount of hydropower in the grid also reduces stress in the transmission
 407 line, a point illustrated by the frequency of N-1 violations. There are, in particular, three
 408 transmission lines that are periodically stressed, two of which are part of a network that feeds
 409 Phnom Penh, Cambodia’s capital and main load-centre (see Figure 1). The line congestions
 410 are eased as less pressure is placed on the thermal plants to fulfil the high demand. After
 411 the monsoon, the scenarios with forecasts are able to sustain the hydropower production,
 412 allowing more hydropower to be dispatched in the grid as opposed to the scenario without
 413 forecasts.

414 Given these results, it is evident that the use of streamflow forecasts is valuable to
 415 power system operations in terms of (i) reducing hydropower over-production during the
 416 monsoon, (ii) maintaining hydropower supply after the monsoon, and (iii) reducing trans-
 417 mission line stress. Importantly, these points are revealed by the use of a modelling frame-
 418 work accounting for both water and power system dynamics, something that would be
 419 hidden if one were to use a reservoir system model, thereby only focussing on the available
 420 hydropower. This highlights the complexity of the coupled water-energy system and the
 421 importance of exploring the multiple roles played by forecasts as we move beyond a water
 422 reservoir system.

423 *5.1.2 Intra- and inter-annual variability of forecast value*

424 Better understanding the inter- and intra-annual variability of forecast value can pro-
 425 vide a deeper insight into when and why forecasts matter to grid operations in hydro-
 426 dominated power systems. To support this analysis, we focus solely on dispatched hy-
 427 dropower (which largely affects the power generation mix), and introduce a metric defined
 428 as the difference between the hydropower dispatched by each forecast-informed scheme and
 429 the one dispatched when adopting rule curves. Hence, positive values mean that a forecast-
 430 informed scheme performs better than rule curves. The values illustrated in Figure 4 reveal

431 a few interesting insights. First, the benefit associated to forecasts is most of the time neg-
 432 ative between February and October, meaning that forecasts are in general not beneficial
 433 during the pre-monsoon and monsoon seasons. This is in contrast to the period between
 434 November and January (post-monsoon season), when positive benefits are observed. Second,
 435 positive benefits extend to almost 200 GWh/month, while the negative ones to less than
 436 -100 GWh/month. This indicates that the extent of benefits derived from using forecast-
 437 informed schemes, albeit less frequent, is more significant. Third, there are a few instances
 438 in which positive benefits are observed during the the pre-monsoon and monsoon seasons
 439 (e.g., April 2007, June 2010, July 2004). These episodes are due to specific, and unexpected,
 440 fluctuations in dam inflow for that particular year. In 2007, for instance, the 30-day outlook
 441 shows that the inflow will keep increasing in May, therefore the reservoirs release more water
 442 and produce more hydropower, which is then dispatched into the grid (refer to Figure S4 in
 443 the SI). This information is unknown to the scheme without forecast, explaining the larger
 444 benefits derived in April 2007.

445 Looking at the inter-annual variability, our results show that the three best and worst
 446 performing years are 2000, 2001, 2018, and 2002, 2005, and 2008, respectively. A closer look
 447 at the reservoir inflow corresponding to each year, shown in Figure 5, gives us two insights
 448 regarding the hydrological conditions that are favorable to forecast-informed schemes. First,
 449 larger inflow volumes tend to be beneficial. Second, and perhaps more interesting, forecasts
 450 are more useful when the inflow patterns present sudden and unexpected changes; a situation
 451 that can be hardly managed when controlling a reservoir system with rule curves.

452 5.2 Skill-value relationship

453 To understand how forecast value changes with skill, we conducted deterministic sim-
 454 ulations using the 11 individual streamflow forecast members. We then investigate the
 455 skill-value relationship under two reservoir operating schemes: (i) without (Section 5.2.1)
 456 and (ii) with (Section 5.2.2) feedback between the reservoir and power systems. This al-
 457 lows us to characterize the skill-value relationship under different levels of integration of the
 458 coupled water-energy system.

459 5.2.1 System operations without feedback

460 To study the relationship between forecast skill and value, we define skill using the
 461 forecast error (Section 4) and relate it to difference performance metrics that character-
 462 ize forecast value, namely available, dispatched, and unused hydropower, system operating
 463 costs, CO₂ emissions, and number of N-1 violations. In our analysis, we also consider
 464 two additional variables, or stressors, that may affect system performance. These are the
 465 inflow to the reservoirs and electricity demand, or load. All these variables are then ana-
 466 lyzed through a correlation matrix and a multiple linear regression model, whose results are
 467 reported Figure 6.

468 Beginning with the correlation analysis (left panel), our results show that the corre-
 469 lation between stressors and performance is significant ($p < 0.05$) for most stressor-metric
 470 pairs. Beginning with the forecast error, we note two important patterns. First, there is a
 471 strong negative correlation between error and available and dispatched hydropower, meaning
 472 that, as the error increases, the contribution of hydropower to the generation mix decreases.
 473 In turn, this explains the positive correlation with costs, CO₂ emissions, and N-1 violations
 474 (recall that the power system must rely more on thermolectric power and imports when less
 475 hydropower is available). Second, the strength of the relationship between forecast error and
 476 performance metrics decreases as we move from the reservoir system to the power system,
 477 a result that is explained by the fact that other stressors become relevant when studying
 478 coupled water-energy systems. Inflow, for instance, positively affects hydropower-related
 479 and negatively affects costs, CO₂ emissions, and grid stress. An increase in load, on the
 480 other hand, implies an increase in costs and CO₂ emissions.

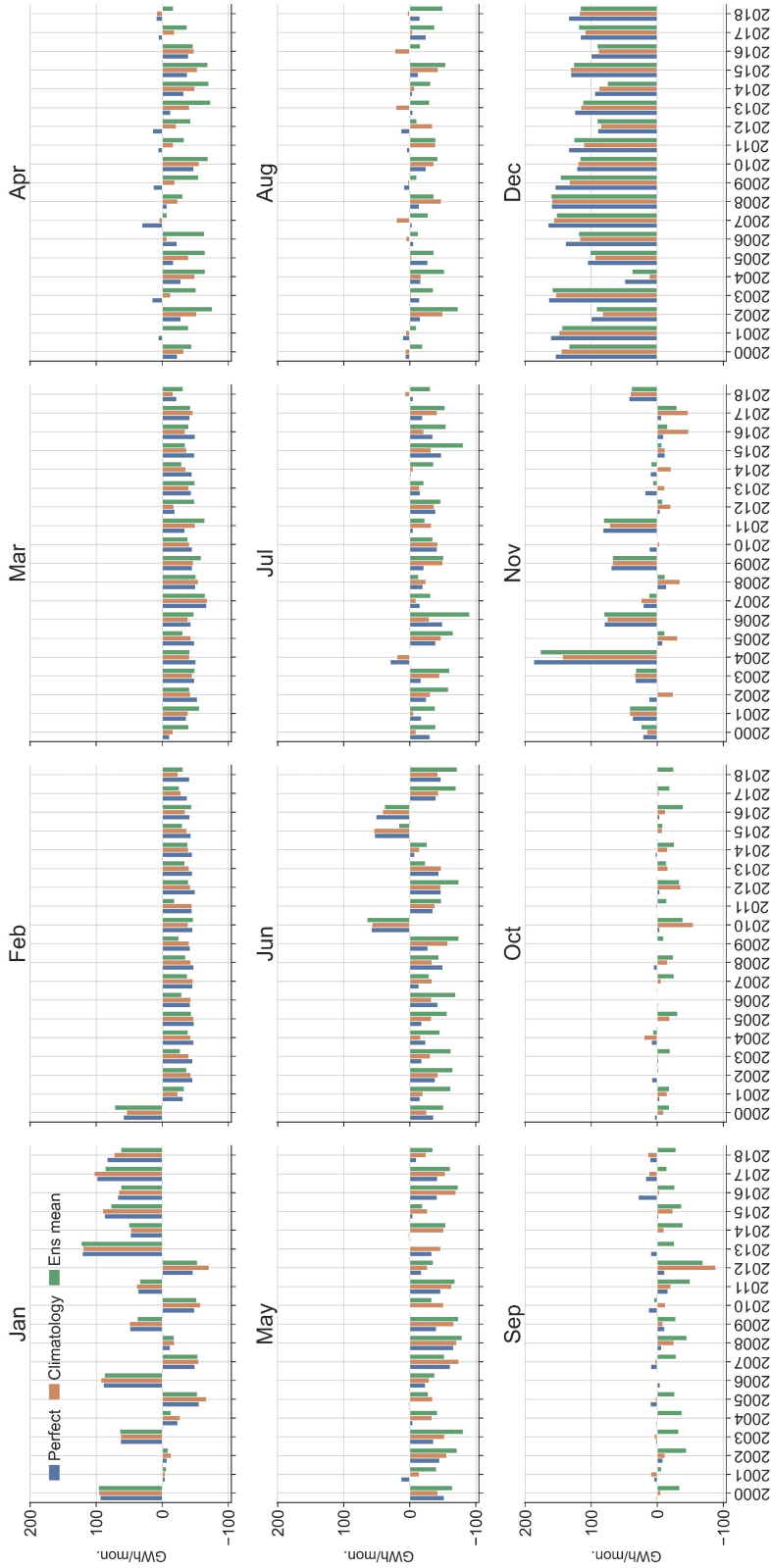


Figure 4. Benefit of using streamflow forecasts at different times of the year, defined as the difference between the amount of hydropower dispatched with and without forecast. The results are grouped according to calendar months (12 panels) and year (horizontal axis). Each cluster of three bars represents the three forecast-informed schemes: perfect forecasts, climatology, and ensemble mean. The values shown are the positive/negative benefits of using each kind of forecast, i.e., the difference between the hydropower dispatched by each forecast-informed scheme and the one dispatched when adopting rule curves.

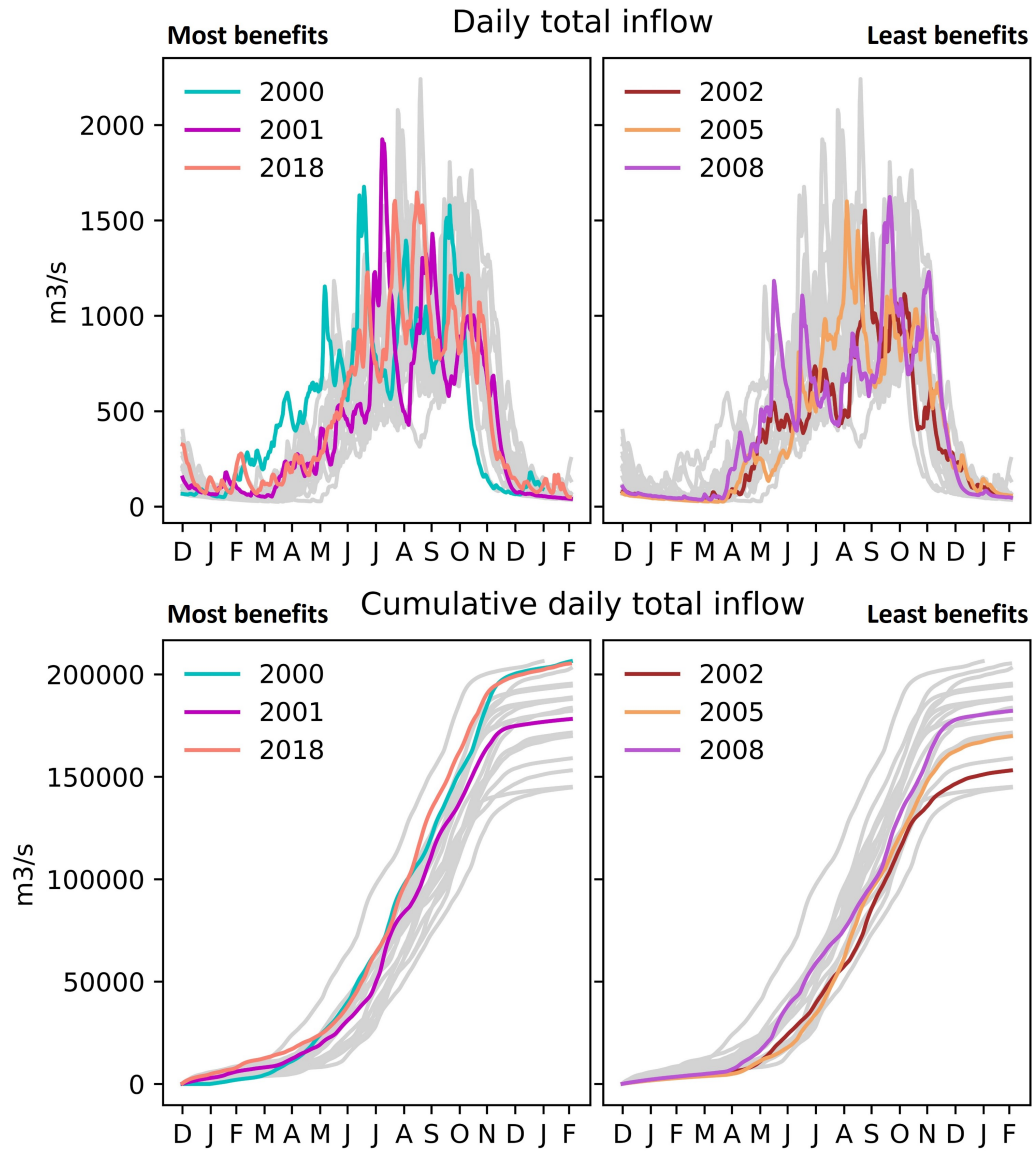


Figure 5. Comparison of daily time series (top panels) and cumulative (bottom panels) inflow profiles across different years. Each gray line represents one year between 2000 and 2018. Based on the total hydropower dispatched each year, three years with the highest and lowest benefits are identified and highlighted in the left and right panels, respectively.

481 To further understand how forecast error, inflow, and load control the performance
 482 metrics, we identify multiple linear regression models in which the inputs are the significant
 483 independent variables (predictors) and each of the six metrics are the dependent variables
 484 (predictands). All variables are first standardized (by subtracting the variable’s mean from
 485 each observed value and then dividing by the variable’s standard deviation) to facilitate the
 486 comparison. Using a forward selection approach, the predictors are iteratively added to the
 487 regression model, beginning from the one with the highest (absolute value of) correlation
 488 coefficient r (Galelli, Humphrey, et al., 2014). From the model, the coefficient of determina-
 489 tion (r^2) and final regression coefficients allow us to infer the contribution of each predictor
 490 to the variance of the predictands, and hence the importance of the model inputs. The
 491 variables are grouped according to the calendar months before carrying out the regression.
 492 The results are illustrated in the central and right panels of Figure 6.

493 Similar to the previous analyses, this analysis can also be organized around three
 494 periods, i.e., pre-monsoon, monsoon and post-monsoon. The importance of the forecast
 495 error for the available hydropower is more obvious during the post-monsoon season, since
 496 a discrepancy between observed and predicted inflow determines how well the system can
 497 adapt to foreseen changes in reservoir inflow and overall transition into the dry season.
 498 This is in contrast to the monsoon season, when the reservoirs usually release close to the
 499 maximum designed release, reducing the importance of forecast errors. Moving to the next
 500 metric, the dispatched hydropower is determined through power system operations. During
 501 the pre-monsoon, less hydropower is produced, and whatever is produced usually gets fully
 502 utilized. The importance of inflow and error to hydropower usage is thus similar to that
 503 of hydropower production between February and April. During the monsoon, however, the
 504 abundant hydropower production forces the electricity demand to be the limiting factor for
 505 the amount of dispatched hydropower, explaining the importance of load during this period.
 506 Regardless of the error or inflow, the power system constraints dictate the grid usage. The
 507 dynamics between the available and dispatched hydropower also directly influence the next
 508 metric, i.e., the unused hydropower. As seen from the regression coefficients, a reduction
 509 in load can create a more than proportionate increase in the amount of unused hydro. The
 510 over-production peaks in October across all forecast-informed schemes, with about 30%
 511 unused hydro. Figure 6 also suggests that the forecast errors become insignificant beyond
 512 the first two performance metrics, since the power system performance depends primarily
 513 on inflow and load.

514 Breaking down the relative contributions of forecast errors, reservoir inflow, and elec-
 515 tricity demand to different performance metrics highlights the complexity of the systems
 516 and the interdependencies between stressors. Streamflow forecasts are most valuable to
 517 improving power system performance during the post-monsoon by facilitating a smooth
 518 transition between the monsoon and post-monsoon seasons. A more accurate forecast al-
 519 lows resources to be exploited for continued hydropower availability for the grid to dispatch.
 520 As we move from the water system to the power system, the skill-value relationship becomes
 521 less significant, as the system responses depend more on the electricity demand.

522 **5.2.2 System operations with feedback**

523 The operations of the reservoir and power systems may not be entirely independent.
 524 To characterize the skill-value relationship under a tighter integration of the two systems,
 525 we repeat all experiments with the same inputs, but this time adding the feedback between
 526 the power and reservoir systems. This set of experiments thus makes use of the re-operation
 527 module described in Section 3.4. Using the same methodology described in Section 5.2.1,
 528 we study the relationship between the system stressors and performance metrics illustrated
 529 in Figure 7.

530 With the re-operation mechanism in place, the role played by electricity demand is am-
 531 plified, while the importance of forecast skill (error) and reservoir inflow is largely reduced.

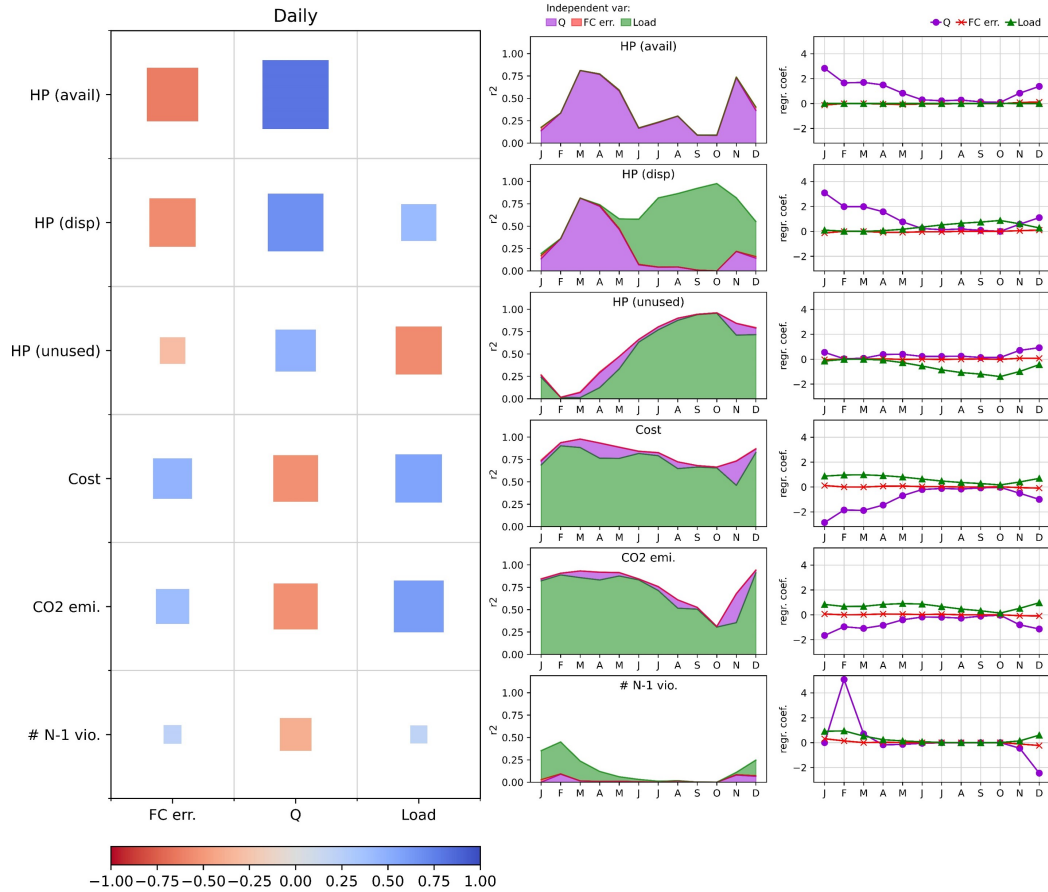


Figure 6. Relationship between system stressors (forecast error, inflow, and load) and performance metrics (available, dispatched, and unused hydropower, system operating costs, CO₂ emissions, and number of N-1 violations) illustrated by a correlation matrix (left) and regression model results (center and right). In the correlation matrix, the values (shown in the color bar) between each stressor-metric pair are obtained by bootstrapping the data through 1,000 iterations. Based on the correlation values, we first identify a multiple linear regression model between the stressors (predictors) and metrics (predictands), and then estimate the contribution of each predictor to the explained variance (center) and the corresponding regression coefficients (right). These results are reported for the scenarios that do not include the feedback between the power and water system.

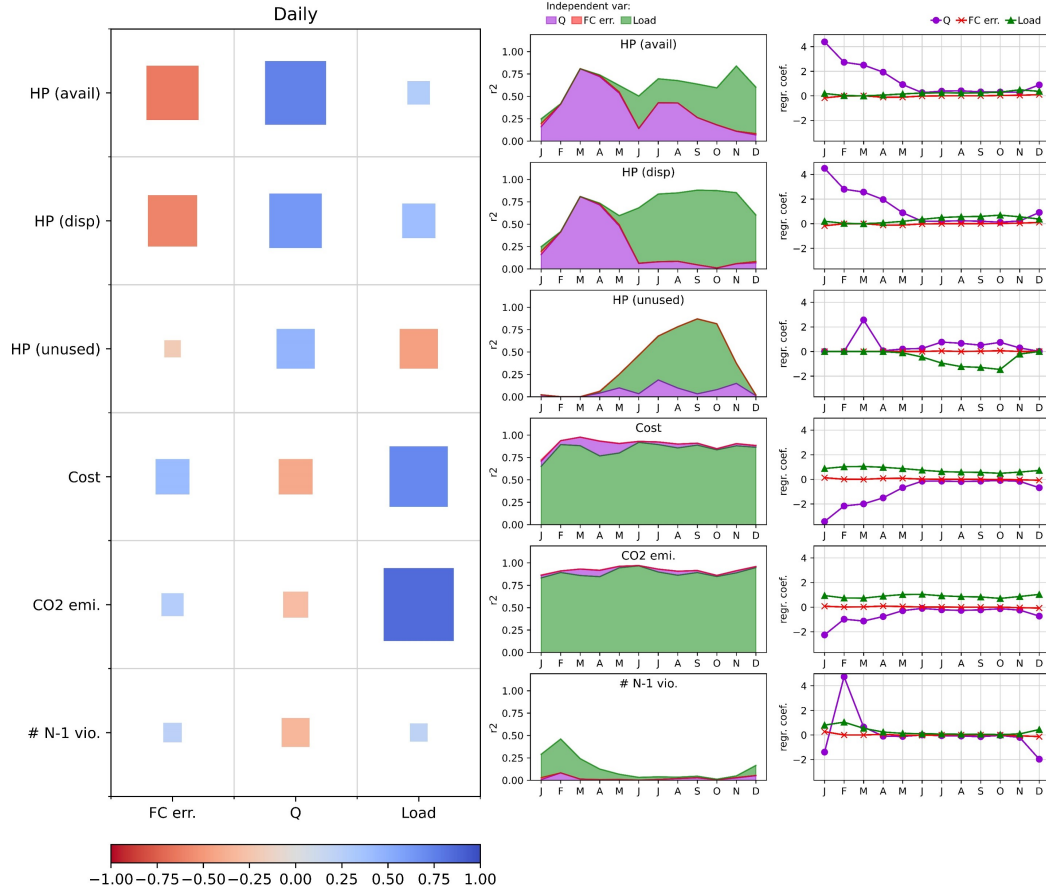


Figure 7. Relationship between system stressors (forecast error, inflow, and load) and performance metrics (available, dispatched, and unused hydropower, system operating costs, CO₂ emissions, and number of N-1 violations). These results are reported for the scenarios that include the feedback between the power and water system.

532 As the goal of the re-operation mechanism is to flexibly store and release water to generate
 533 hydropower that better matches the power system demand, the reservoir storage patterns
 534 can largely deviate from the seasonal patterns (Koh et al., 2022). In turn, this partially
 535 dampens the impact of hydrological variability on power system performance, making both
 536 inflow and forecast skill less important. With hydropower-related metrics being explained
 537 by load, it follows that operating costs and CO₂ emissions can almost entirely be determined
 538 by load as well, with r^2 values close to one for every month. Evidently, the presence of the
 539 feedback mechanism reduces the value of forecasts, allowing load to dominate the operating
 540 decisions in both the reservoirs and power system.

541 6 Discussion and conclusions

542 Our study evaluates the value of streamflow forecasts in hydro-dominated power systems.
 543 The performance metrics were selected from both the reservoir and power systems to
 544 represent the hydropower generation by the reservoirs, hydropower usage within the grid,
 545 as well as economic, environmental, and reliability aspects of the power system. We show that
 546 defining forecast value in terms of different performance metrics can produce different
 547 outcomes. For instance, while previous studies often associate favorable forecasts with greater

548 hydropower availability, we found that larger hydropower availability does not necessarily
 549 translate into more usage within the grid. Unless the excess water release can serve a second
 550 purpose—such as for groundwater storage (Nayak et al., 2018) or inter-basin transfer (Li et
 551 al., 2014)—measuring value only in terms of the available hydropower may thus overlook
 552 other important aspects, such as production costs or CO₂ emissions. Therefore, when we
 553 study hydropower systems, we should consider the role that hydropower reservoirs play, not
 554 only within the reservoir network, but also within the power system as well.

555 In hydro-dominated power systems, hydropower operations are highly influenced by
 556 the seasonality of reservoir inflow. As a result, the grid operations and performance exhibit
 557 a strong seasonal profile as well. In our case study, the system behavior can be classified
 558 into three periods—pre-monsoon, monsoon and post-monsoon. We show that the value
 559 of streamflow forecasts varies with these different periods. During the monsoon, the use
 560 of forecasts reduces hydropower over-production. In the post-monsoon season, operating
 561 with forecasts is beneficial to sustain hydropower supply. Accurate forecasts are especially
 562 useful during the three months after the end of the monsoon to facilitate the transition from
 563 wet to dry seasons. Better forecast skill, combined with large inflow conditions, can thus
 564 benefit the system in terms of larger dispatched hydropower, lowering operating costs and
 565 CO₂ emissions. Our analysis also shows that, with a tighter integration of the reservoir
 566 and power systems, the role played by electricity demand becomes dominant in determining
 567 operational decisions within both systems.

568 Looking forward, an important aspect warranting additional research is the impact of
 569 the uncertainty associated to streamflow forecasts, which could be ‘operationalized’ through
 570 the use of stochastic MPC schemes (Pianosi & Soncini-Sessa, 2009). Such control schemes
 571 would become particularly useful when dealing with streamflow forecasts spanning across
 572 longer timescales than those currently available for this region. Another relevant aspect to
 573 consider in the future is the integration of other forms of forecasts that could improve the
 574 operation of water-energy systems, such as electric load forecasts (Hong & Fan, 2016).

575 Overall, we believe that a better understanding of the value provided by streamflow
 576 forecasts to multi-sector infrastructures could promote and support their use. The need for
 577 better approaches to system operations is indeed necessary in a variety of contexts, from
 578 regions experiencing hydro-climatological shifts to regions, like Southeast Asia, that are
 579 expanding their water and power supply networks.

580 Notation

581 S_d^i Storage on day d of the i -th reservoir

582 S_{cap}^i Capacity of the i -th reservoir

583 R_d^i Volume of water released through the turbines of the i -th reservoir on day d

584 R_{max}^i Maximum volume of water that can be turbined from the i -th reservoir

585 Q_d^i Inflow on day d to the i -th reservoir

586 $Q_{MEF,d}^i$ Downstream environmental flow requirement of the i -th reservoir on day d

587 $spill_d^i$ Volume of water spilled from the i -th reservoir on day d

588 E_d^i Evaporation losses from the i -th reservoir on day d

589 HP_d^i Available hydropower on day d from the i -th reservoir

590 HP_t^{i*} Hydropower dispatched in hour t from the i -th reservoir

591 H_d^i Hydraulic head from the i -th reservoir on day d

592 Open Research Section

593 The data and Python scripts used to simulate the water-energy system in Cambodia for
 594 this research are available at Koh (2023) via <https://doi.org/10.5281/zenodo.8163034>.

595 The observed reservoir inflow data are available from <https://doi.org/10.24381/cds>
 596 [.a4fdd6b9](https://doi.org/10.24381/cds) (Harrigan et al., 2021) and the reservoir inflow forecast data are available from
 597 <https://doi.org/10.24381/cds>.2d78664e (Zsoter et al., 2020). Power system paramete-
 598 rers, including generator and transmission line specifications, as well as monthly electricity
 599 peak demand data are extracted from EDC (2016) and JICA (2014).

600 Acknowledgments

601 Rachel Koh is supported by the President’s Graduate Fellowship from the Singapore Uni-
 602 versity of Technology and Design.

603 References

- 604 Ahmad, S., & Hossain, F. (2020). Maximizing energy production from hydropower dams
 605 using short-term weather forecasts. *Renewable Energy*, *146*, 1560–1577.
- 606 Anghileri, D., Monhart, S., Zhou, C., Bogner, K., Castelletti, A., Burlando, P., & Zappa,
 607 M. (2019). The value of subseasonal hydrometeorological forecasts to hydropower
 608 operations: How much does preprocessing matter? *Water Resources Research*, *55*(12),
 609 10159–10178.
- 610 Anghileri, D., Voisin, N., Castelletti, A., Pianosi, F., Nijssen, B., & Lettenmaier, D. (2016).
 611 Value of long-term streamflow forecasts to reservoir operations for water supply in
 612 snow-dominated river catchments. *Water Resources Research*, *52*(6), 4209–4225.
- 613 Chowdhury, A. K., Dang, T. D., Bagchi, A., & Galelli, S. (2020). Expected benefits
 614 of Laos’ hydropower development curbed by hydroclimatic variability and limited
 615 transmission capacity: Opportunities to reform. *Journal of Water Resources Planning
 616 and Management*, *146*(10), 05020019.
- 617 Chowdhury, A. K., Dang, T. D., Nguyen, H., Koh, R., & Galelli, S. (2021). The Greater
 618 Mekong’s climate-water-energy nexus: How ENSO-triggered regional droughts affect
 619 power supply and CO₂ emissions. *Earth’s Future*, *9*(3).
- 620 Chowdhury, A. K., Kern, J., Dang, T. D., & Galelli, S. (2020). PowNet: A network-
 621 constrained unit commitment/economic dispatch model for large-scale power systems
 622 analysis. *Journal of Open Research Software*, *8*(1).
- 623 Dang, T. D., Vu, D. T., Chowdhury, A. K., & Galelli, S. (2020). A software package for the
 624 representation and optimization of water reservoir operations in the VIC hydrologic
 625 model. *Environmental Modelling and Software*, *126*.
- 626 Delaney, C., Hartman, R., Mendoza, J., Dettinger, M., Delle Monache, L., Jasperse, J., ...
 627 Evett, S. (2020). Forecast informed reservoir operations using ensemble streamflow
 628 predictions for a multipurpose reservoir in Northern California. *Water Resources
 629 Research*, *56*(9), e2019WR026604.
- 630 Ding, Z., Wen, X., Tan, Q., Yang, T., Fang, G., Lei, X., ... Wang, H. (2021). A forecast-
 631 driven decision-making model for long-term operation of a hydro-wind-photovoltaic
 632 hybrid system. *Applied Energy*, *291*, 116820.
- 633 Doering, K., Quinn, J., Reed, P., & Steinschneider, S. (2021). Diagnosing the time-varying
 634 value of forecasts in multiobjective reservoir control. *Journal of Water Resources
 635 Planning and Management*, *147*(7), 04021031.
- 636 EDC. (2016). *Annual Report 2016* (Tech. Rep.). Electricité du Cambodge (EDC).
- 637 Galelli, S., Dang, T. D., Ng, J. Y., Chowdhury, A. K., & Arias, M. E. (2022). Opportu-
 638 nities to curb hydrological alterations via dam re-operation in the mekong. *Nature
 639 Sustainability*, *5*(12), 1058–1069.
- 640 Galelli, S., Goedbloed, A., Schwanenberg, D., & van Overloop, P. (2014). Optimal real-
 641 time operation of multipurpose urban reservoirs: Case study in Singapore. *Journal of
 642 Water Resources Planning and Management*, *140*(4), 511–523.
- 643 Galelli, S., Humphrey, G. B., Maier, H. R., Castelletti, A., Dandy, G. C., & Gibbs, M. S.
 644 (2014). An evaluation framework for input variable selection algorithms for environ-
 645 mental data-driven models. *Environmental Modelling & Software*, *62*, 33–51.

- 646 Gebretsadik, Y., Fant, C., Strzepek, K., & Arndt, C. (2016). Optimized reservoir operation
647 model of regional wind and hydro power integration case study: Zambezi basin and
648 South Africa. *Applied Energy*, *161*, 574–582.
- 649 Gong, Y., Liu, P., Ming, B., & Li, D. (2021). Identifying the effect of forecast uncertainties
650 on hybrid power system operation: A case study of Longyangxia hydro–photovoltaic
651 plant in China. *Renewable Energy*, *178*, 1303–1321.
- 652 Grantz, K., Rajagopalan, B., Clark, M., & Zagona, E. (2005). A technique for incorporating
653 large-scale climate information in basin-scale ensemble streamflow forecasts. *Water
654 Resources Research*, *41*(10).
- 655 Guo, Y., Xu, Y., Xie, J., Chen, H., Si, Y., & Liu, J. (2021). A weights combined model for
656 middle and long-term streamflow forecasts and its value to hydropower maximization.
657 *Journal of Hydrology*, *602*, 126794.
- 658 Harrigan, S., Zsoter, E., Barnard, C., Wetterhall, F., Ferrario, I., Mazzetti, C., . . . Prud-
659 homme, C. (2021). *River discharge and related historical data from the Global Flood
660 Awareness System, v3.1, Copernicus Climate Change Service (C3S) Climate Data
661 Store (CDS)*. Retrieved from <https://doi.org/10.24381/cds.a4fdd6b9>
- 662 Hong, T., & Fan, S. (2016). Probabilistic electric load forecasting: A tutorial review.
663 *International Journal of Forecasting*, *32*(3), 914–938.
- 664 Huang, Z., & Zhao, T. (2022). Predictive performance of ensemble hydroclimatic forecasts:
665 Verification metrics, diagnostic plots and forecast attributes. *Wiley Interdisciplinary
666 Reviews: Water*, *9*(2), e1580.
- 667 Ibanez, E., Magee, T., Clement, M., Brinkman, G., Milligan, M., & Zagona, E. (2014).
668 Enhancing hydropower modeling in variable generation integration studies. *Energy*,
669 *74*, 518–528.
- 670 JICA. (2014). *Preparatory survey for Phnom Penh city transmission and distribution sys-
671 tem expansion project phase II in the Kingdom of Cambodia* (Tech. Rep.). Japan
672 International Cooperation Agency (JICA).
- 673 Kern, J. D., Su, Y., & Hill, J. (2020). A retrospective study of the 2012–2016 California
674 drought and its impacts on the power sector. *Environmental Research Letters*, *15*(9).
- 675 Koh, R. (2023). PowNetRes_FC: Initial release (v1.0). Zenodo. [Dataset and Software].
676 Retrieved from <https://doi.org/10.5281/zenodo.8163034>
- 677 Koh, R., Kern, J., & Galelli, S. (2022). Hard-coupling water and power system models
678 increases the complementarity of renewable energy sources. *Applied Energy*, *321*,
679 119386.
- 680 Lee, D., Ng, J., Galelli, S., & Block, P. (2022). Unfolding the relationship between seasonal
681 forecast skill and value in hydropower production: A global analysis. *Hydrology and
682 Earth System Sciences*, *26*(9), 2431–2448.
- 683 Li, W., Sankarasubramanian, A., Ranjithan, R., & Brill, E. (2014). Improved regional
684 water management utilizing climate forecasts: An interbasin transfer model with a
685 risk management framework. *Water Resources Research*, *50*(8), 6810–6827.
- 686 Lima, C., & Lall, U. (2010). Climate informed monthly streamflow forecasts for the Brazilian
687 hydropower network using a periodic ridge regression model. *Journal of hydrology*,
688 *380*(3–4), 438–449.
- 689 Liu, P., Guo, S., Xu, X., & Chen, J. (2011). Derivation of aggregation-based joint operating
690 rule curves for cascade hydropower reservoirs. *Water Resources Management*, *25*,
691 3177–3200.
- 692 MacLeod, D., Easton-Calabria, E., de Perez, E., & Jaime, C. (2021). Verification of forecasts
693 for extreme rainfall, tropical cyclones, flood and storm surge over Myanmar and the
694 Philippines. *Weather and climate extremes*, *33*, 100325.
- 695 McInerney, D., Thyer, M., Kavetski, D., Laugesen, R., Tuteja, N., & Kuczera, G. (2020).
696 Multi-temporal hydrological residual error modeling for seamless subseasonal stream-
697 flow forecasting. *Water Resources Research*, *56*(11), e2019WR026979.
- 698 Nash, J. E., & Sutcliffe, J. V. (1970). River flow forecasting through conceptual models
699 part I—A discussion of principles. *Journal of hydrology*, *10*(3), 282–290.
- 700 Nayak, M., Herman, J., & Steinschneider, S. (2018). Balancing flood risk and water supply

- in California: Policy search integrating short-term forecast ensembles with conjunctive use. *Water Resources Research*, *54*(10), 7557–7576.
- Ogliari, E., Guilizzoni, M., Giglio, A., & Pretto, S. (2021). *Renewable Energy*, *178*, 1466–1474.
- Oliveira, R., & Loucks, D. (1997). Operating rules for multireservoir systems. *Water Resources Research*, *33*(4), 839–852.
- Pastor, A. V., Ludwig, F., Biemans, H., Hoff, H., & Kabat, P. (2014). Accounting for environmental flow requirements in global water assessments. *Hydrology and Earth System Sciences*, *18*(12), 5041–5059.
- Pianosi, F., & Soncini-Sessa, R. (2009). Real-time management of a multipurpose water reservoir with a heteroscedastic inflow model. *Water Resources Research*, *45*(10).
- Quedi, E., & Fan, F. (2020). Sub seasonal streamflow forecast assessment at large-scale basins. *Journal of Hydrology*, *584*, 124635.
- Slater, L. J., Villarini, G., Bradley, & A., A. (2016). Evaluation of the skill of north-American multi-model ensemble (NMME) global climate models in predicting average and extreme precipitation and temperature over the continental USA. *Climate Dynamics*, *53*, 7381–7396.
- Soncini-Sessa, R., Weber, E., & Castelletti, A. (2007). *Integrated and participatory water resources management-theory*. Amsterdam, The Netherlands: Elsevier.
- Troin, M., Arsenault, R., Wood, A. W., Brissette, F., & Martel, J.-L. (2021). *Generating ensemble streamflow forecasts: A review of methods and approaches over the past 40 years* (Vol. 56) (No. 7). Wiley Online Library.
- Turner, S., Bennett, J. C., Robertson, D. E., & Galelli, S. (2017). Complex relationship between seasonal streamflow forecast skill and value in reservoir operations. *Hydrology and Earth System Sciences*, *21*(9), 4841–4859.
- Turner, S., Xu, W., & Voisin, N. (2020). Inferred inflow forecast horizons guiding reservoir release decisions across the United States. *Hydrology and Earth System Sciences*, *24*(3), 1275–1291.
- Veloza, O., & Santamaria, F. (2016). Analysis of major blackouts from 2003 to 2015: Classification of incidents and review of main causes. *The Electricity Journal*, *29*(7), 42–49.
- Voisin, N., Dyreson, A., Fu, T., O’Connell, M., Turner, S. W., Zhou, T., & Macknick, J. (2020). Impact of climate change on water availability and its propagation through the Western US power grid. *Applied Energy*, *276*, 115467.
- Voisin, N., Hamlet, A. F., Graham, L. P., Pierce, D. W., Barnett, T. P., & Lettenmaier, D. P. (2006). The role of climate forecasts in Western U.S. power planning. *Journal of Applied Meteorology and Climatology*, *45*(5), 653–673.
- Wang, F., Wang, L., Zhou, H., Saavedra Valeriano, O., Koike, T., & Li, W. (2012). Ensemble hydrological prediction-based real-time optimization of a multiobjective reservoir during flood season in a semiarid basin with global numerical weather predictions. *Water Resources Research*, *48*(7).
- Yassin, F., Razavi, S., Elshamy, M., Davison, B., Sapriza-Azuri, G., & Wheeler, H. (2019). Representation and improved parameterization of reservoir operation in hydrological and land-surface models. *Hydrol. Earth Syst. Sci.*, *23*(9), 3735–3764.
- Yossef, N., Winsemius, H., Weerts, A., van Beek, R., & Bierkens, M. (2013). Skill of a global seasonal streamflow forecasting system, relative roles of initial conditions and meteorological forcing. *Water Resources Research*, *49*(8), 4687–4699.
- Zhao, T., Yang, D., Cai, X., Zhao, J., & Wang, H. (2012). Identifying effective forecast horizon for real-time reservoir operation under a limited inflow forecast. *Water Resources Research*, *48*(1).
- Zimmerman, B., Vimont, D., & Block, P. (2016). Utilizing the state of ENSO as a means for season-ahead predictor selection. *Water Resources Research*, *52*(5), 3761–3774.
- Zsoter, E., Harrigan, S., Barnard, C., Blick, M., Ferrario, I., Wetterhall, F., & Prudhomme, C. (2020). *Reforecasts of river discharge and related data by the Global Flood Awareness System, v2.2, Copernicus Climate Change Service (C3S) Climate Data Store*

(CDS). Retrieved from <https://doi.org/10.24381/cds.2d78664e>